

Immunoassays for the cancer biomarker CA125 based on a large-birefringence nematic liquid-crystal mixture

Shih-Hung Sun,¹ Mon-Juan Lee,^{2,4} Yun-Han Lee,¹ Wei Lee^{1,*} Xiaolong Song,³
and Chao-Yuan Chen³

¹ Institute of Imaging and Biomedical Photonics, College of Photonics, National Chiao Tung University, Guiren Dist., Tainan 71150, Taiwan

² Department of Bioscience Technology, Chang Jung Christian University, Guiren Dist., Tainan 71101, Taiwan

³ Jiangsu Hecheng Display Technology Co., Ltd., Nanjing 210014, China

⁴ mjlee@mail.cjcu.edu.tw (M.-J. Lee)

*wlee@nctu.edu.tw (W. Lee)

Abstract: The use of fluorescence is ubiquitously found in the detection of immunoreaction; though with good sensitivity, this technique requires labeling as well as other time-consuming steps to perform the measurement. An alternative approach involving liquid crystals (LCs) was proposed, based on the fact that an immunocomplex can disturb the orientation of LCs, leading to an optical texture different from the case when only antigen or antibody exists. This method is label-free, easy to manipulate and low-cost. However, its sensitivity was low for practical usage. In this study, we adopted a high-birefringence liquid crystal (LC) to enhance the sensitivity for the immunodetection. Experiments were performed, targeting at the cancer biomarker CA125. We showed that the larger birefringence ($\Delta n = 0.33$ at 20 °C) amplifies the detected signal and, in turn, dramatically improves the detection limit. To avoid signal loss from conventional rinsing steps in immunodetection, CA125 antigen and antibody were reacted before immobilized on substrates. We studied the specific binding events and obtained a detection limit as low as 1 ng/ml. The valid temperature ranges were compared by using the typical single-compound LC 5CB and the high-birefringence LC mixture. We further investigated time dependency of the optical textures and affirmed the capability of LC-based immunodetection in distinguishing between specific and nonspecific antibodies.

©2014 Optical Society of America

OCIS codes: (160.3710) Liquid crystals; (170.0170) Medical optics and biotechnology.

References and links

1. N. Scholler and N. Urban, "CA125 in ovarian cancer," *Biomarkers Med.* **1**(4), 513–523 (2007).
2. N. Kui Wong, R. L. Easton, M. Panico, M. Sutton-Smith, J. C. Morrison, F. A. Lattanzio, H. R. Morris, G. F. Clark, A. Dell, and M. S. Patankar, "Characterization of the oligosaccharides associated with the human ovarian tumor marker CA125," *J. Biol. Chem.* **278**(31), 28619–28634 (2003).
3. M. S. Patankar, Y. Jing, J. C. Morrison, J. A. Belisle, F. A. Lattanzio, Y. Deng, N. K. Wong, H. R. Morris, A. Dell, and G. F. Clark, "Potent suppression of natural killer cell response mediated by the ovarian tumor marker CA125," *Gynecol. Oncol.* **99**(3), 704–713 (2005).
4. A. Berruti, M. Tampellini, M. Torta, T. Buniva, G. Gorzegno, and L. Dogliotti, "Prognostic value in predicting overall survival of two mucinous markers: CA 15-3 and CA 125 in breast cancer patients at first relapse of disease," *Eur. J. Cancer* **30**(14), 2082–2084 (1994).
5. L. F. Norum, B. Erikstein, and K. Nustad, "Elevated CA125 in breast cancer--A sign of advanced disease," *Tumour Biol.* **22**(4), 223–228 (2001).
6. M. Yamamoto, H. Baba, Y. Toh, T. Okamura, and Y. Maehara, "Peritoneal lavage CEA/CA125 is a prognostic factor for gastric cancer patients," *J. Cancer Res. Clin. Oncol.* **133**(7), 471–476 (2007).
7. B. Zhang, F. F. Cai, and X. Y. Zhong, "An overview of biomarkers for the ovarian cancer diagnosis," *Eur. J.*

- Obstet. Gynecol. Reprod. Biol. **158**(2), 119–123 (2011).
8. R. C. Bast, Jr., M. Feeney, H. Lazarus, L. M. Nadler, R. B. Colvin, and R. C. Knapp, "Reactivity of a monoclonal antibody with human ovarian carcinoma," *J. Clin. Invest.* **68**(5), 1331–1337 (1981).
 9. R. Madiyalakan, M. Kuzma, A. A. Noujaim, and M. R. Suresh, "An antibody-lectin sandwich assay for the determination of CA125 antigen in ovarian cancer patients," *Glycoconj. J.* **13**(4), 513–517 (1996).
 10. J. Wang and J. Ren, "A sensitive and rapid immunoassay for quantification of CA125 in human sera by capillary electrophoresis with enhanced chemiluminescence detection," *Electrophoresis* **26**(12), 2402–2408 (2005).
 11. S. Suwansa-ard, P. Kanatharana, P. Asawatreratanakul, B. Wongkittisuksa, C. Limsakul, and P. Thavarungkul, "Comparison of surface plasmon resonance and capacitive immunosensors for cancer antigen 125 detection in human serum samples," *Biosens. Bioelectron.* **24**(12), 3436–3441 (2009).
 12. H. A. Huckabay and R. C. Dunn, "Whispering gallery mode imaging for the multiplexed detection of biomarkers," *Sens. Actuators B Chem.* **160**(1), 1262–1267 (2011).
 13. H. A. Huckabay, S. M. Wildgen, and R. C. Dunn, "Label-free detection of ovarian cancer biomarkers using whispering gallery mode imaging," *Biosens. Bioelectron.* **45**, 223–229 (2013).
 14. M. A. Bangar, D. J. Shirale, W. Chen, N. V. Myung, and A. Mulchandani, "Single conducting polymer nanowire chemiresistive label-free immunosensor for cancer biomarker," *Anal. Chem.* **81**(6), 2168–2175 (2009).
 15. H.-K. Chang, F. N. Ishikawa, R. Zhang, R. Datar, R. J. Cote, M. E. Thompson, and C. Zhou, "Rapid, label-free, electrical whole blood bioassay based on nanobiosensor systems," *ACS Nano* **5**(12), 9883–9891 (2011).
 16. A. Singh, S. Park, and H. Yang, "Glucose-oxidase label-based redox cycling for an incubation period-free electrochemical immunosensor," *Anal. Chem.* **85**(10), 4863–4868 (2013).
 17. D. Tang, R. Yuan, and Y. Chai, "Magnetic control of an electrochemical microfluidic device with an arrayed immunosensor for simultaneous multiple immunoassays," *Clin. Chem.* **53**(7), 1323–1329 (2007).
 18. A. Kim, C. S. Ah, C. W. Park, J. H. Yang, T. Kim, C. G. Ahn, S. H. Park, and G. Y. Sung, "Direct label-free electrical immunodetection in human serum using a flow-through-apparatus approach with integrated field-effect transistors," *Biosens. Bioelectron.* **25**(7), 1767–1773 (2010).
 19. K. W. Kim, J. Song, J. S. Kee, Q. Liu, G. Q. Lo, and M. K. Park, "Label-free biosensor based on an electrical tracing-assisted silicon microring resonator with a low-cost broadband source," *Biosens. Bioelectron.* **46**, 15–21 (2013).
 20. E. Stern, A. Vacic, N. K. Rajan, J. M. Criscione, J. Park, B. R. Ilic, D. J. Mooney, M. A. Reed, and T. M. Fahmy, "Label-free biomarker detection from whole blood," *Nat. Nanotechnol.* **5**(2), 138–142 (2010).
 21. G. J. Zhang and Y. Ning, "Silicon nanowire biosensor and its applications in disease diagnostics: a review," *Anal. Chim. Acta* **749**, 1–15 (2012).
 22. T. Zhang, Y. He, J. Wei, and L. Que, "Nanostructured optical microchips for cancer biomarker detection," *Biosens. Bioelectron.* **38**(1), 382–388 (2012).
 23. P. S. Cremer, "Label-free detection becomes crystal clear," *Nat. Biotechnol.* **22**(2), 172–173 (2004).
 24. S. J. Woltman, G. D. Jay, and G. P. Crawford, "Liquid-crystal materials find a new order in biomedical applications," *Nat. Mater.* **6**(12), 929–938 (2007).
 25. A. Hussain, A. S. Pina, and A. C. Roque, "Bio-recognition and detection using liquid crystals," *Biosens. Bioelectron.* **25**(1), 1–8 (2009).
 26. J. M. Brake, M. K. Daschner, Y. Y. Luk, and N. L. Abbott, "Biomolecular interactions at phospholipid-decorated surfaces of liquid crystals," *Science* **302**(5653), 2094–2097 (2003).
 27. Y.-Y. Luk, M. L. Tingey, K. A. Dickson, R. T. Raines, and N. L. Abbott, "Imaging the binding ability of proteins immobilized on surfaces with different orientations by using liquid crystals," *J. Am. Chem. Soc.* **126**(29), 9024–9032 (2004).
 28. M. L. Tingey, S. Wilyana, E. J. Snodgrass, and N. L. Abbott, "Imaging of affinity microcontact printed proteins by using liquid crystals," *Langmuir* **20**(16), 6818–6826 (2004).
 29. B. H. Clare and N. L. Abbott, "Orientations of nematic liquid crystals on surfaces presenting controlled densities of peptides: amplification of protein-peptide binding events," *Langmuir* **21**(14), 6451–6461 (2005).
 30. X. Bi, S. L. Lai, and K.-L. Yang, "Liquid crystal multiplexed protease assays reporting enzymatic activities as optical bar charts," *Anal. Chem.* **81**(13), 5503–5509 (2009).
 31. J. Hoogboom, K. Velonia, T. Rasing, A. E. Rowan, and R. J. M. Nolte, "LCD-based detection of enzymatic action," *Chem. Commun. (Camb.)* **2006**(4), 434–435 (2006).
 32. N. A. Lockwood, J. C. Mohr, L. Ji, C. J. Murphy, S. P. Palecek, J. J. de Pablo, and N. L. Abbott, "Thermotropic liquid crystals as substrates for imaging the reorganization of matrigel by human embryonic stem cells," *Adv. Funct. Mater.* **16**(5), 618–624 (2006).
 33. C.-H. Jang, L.-L. Cheng, C. W. Olsen, and N. L. Abbott, "Anchoring of nematic liquid crystals on viruses with different envelope structures," *Nano Lett.* **6**(5), 1053–1058 (2006).
 34. M. K. McCamley, A. W. Arntstein, S. M. Opal, and G. P. Crawford, "Optical detection of sepsis markers using liquid crystal based biosensors," *Proc. SPIE* **6441**, 64411Y (2007).
 35. S.-R. Kim, R. R. Shah, and N. L. Abbott, "Orientations of liquid crystals on mechanically rubbed films of bovine serum albumin: a possible substrate for biomolecular assays based on liquid crystals," *Anal. Chem.* **72**(19), 4646–4653 (2000).
 36. Y.-Y. Luk, C.-H. Jang, L.-L. Cheng, B. A. Israel, and N. L. Abbott, "Influence of lyotropic liquid crystals on the ability of antibodies to bind to surface-immobilized antigens," *Chem. Mater.* **17**(19), 4774–4782 (2005).
 37. C.-Y. Xue, S. A. Khan, and K.-L. Yang, "Exploring optical properties of liquid crystals for developing label-free

- and high-throughput microfluidic immunoassays,” *Adv. Mater.* **21**(2), 198–202 (2009).
38. C.-Y. Xue and K.-L. Yang, “Dark-to-bright optical responses of liquid crystals supported on solid surfaces decorated with proteins,” *Langmuir* **24**(2), 563–567 (2008).
 39. C. H. Chen and K. L. Yang, “Liquid crystal-based immunoassays for detecting hepatitis B antibody,” *Anal. Biochem.* **421**(1), 321–323 (2012).
 40. H.-W. Su, Y.-H. Lee, M.-J. Lee, Y.-C. Hsu, and W. Lee, “Label-free immunodetection of the cancer biomarker CA125 using high- Δn liquid crystals,” *J. Biomed. Opt.* **19**(7), 077006 (2014).
 41. M.-J. Lee, H.-W. Su, S.-H. Sun, and W. Lee, “Ultrahigh sensitivity in liquid-crystal-based immunodetection by surface modification of the alignment layer,” *Proc. SPIE* **9182**, Liquid Crystals XVIII, pp. 91820G (2014).
 42. C.-H. Chen and K.-L. Yang, “Functional protease assay using liquid crystals as a signal reporter,” *Biosens. Bioelectron.* **35**(1), 174–179 (2012).
-

1. Introduction

Detection of cancer biomarkers serves as an important measure in cancer prevention and early screening as well as in cancer diagnosis and prognosis. Cancer biomarkers are proteins or molecules secreted by cancer cells having an increasing level in cancer tissue or serum with the cancer progression. Clinical assays of various cancer biomarkers are therefore established to monitor the early development, progression or possible recurrence of cancer, assessing a patient’s response to cancer treatment and assisting in physical examination. The biomarker CA125, namely, mucin 16 (MUC16), is one of the earliest and most extensively studied biomarkers for cancer [1]. It is expressed as a membrane glycoprotein on cell surface, but may be released as soluble form in blood. CA125 plays a role in cell-mediated immune response, and CA125 derived from tumor cells is suggested to suppress anti-tumor immune response [2,3]. Elevated level of CA125 provides an indication of early- and advanced-stage ovarian cancer, which is also observed in other malignancies such as breast and gastric cancers [4–7].

The level of CA125 is commonly determined by a sandwich assay—an immunoassay based on the specific binding of the CA125 antigen by two types of anti-CA125 primary antibodies, followed by detection with a fluorescence-labeled or enzyme-conjugated secondary antibody [8–10]. The immunodetection is also achieved by labeling one of the primary antibodies with fluorophores, thus eliminating the use of secondary antibodies. Although extensively applied in biochemical analysis, one of the disadvantages of sandwich assays is the unavailability of matched pairs of primary antibodies, which must recognize different epitopes on the antigen so that the binding of each individual antibody is not hindered by its counterpart. Another drawback of label-based assays lies in the labeling procedure, which often involves chemical modification that may affect the activity or binding efficiency of the labeled antibody. The use of labeling reagents and the reaction of antigen–antibody immunocomplexes with labeled antibodies also increase the cost and time of the assay. Furthermore, cross-reactivity of secondary antibody with antigen is an issue that may result in nonspecific binding and false-positive results. Consequently, various label-free assays are developed to simplify the immunodetection procedure without the use of labeled antibodies. Direct and label-free biosensing approaches such as surface plasmon resonance [11], whispering gallery mode resonance [12,13] and various electrochemical methods [14–17] have been reported to detect CA125 alone or together with several other cancer biomarkers. Other platforms using techniques including silicon nanowires or microchips are designed for label-free detection of cancer biomarkers such as human epidermal growth factor receptor 2 (HER-2), prostate-specific antigen (PSA), carcinoembryonic antigen (CEA) and carcinogenic antigen 15.3 (CA15.3) [18–22].

Liquid crystals (LCs) in their various mesophases are technologically important electro-optical materials as they possess many unique and useful physical and optical properties. Recently, application of LCs in biological sensing has received increasing attention [23,24]. LC-based biosensing exploits the birefringent properties of the anisotropic mesogenic molecules, whose orientation is disturbed in the presence of biomolecules or during the process of a biological event, giving rise to the change in optical appearance of the LC used

[25]. The spontaneous assembly of phospholipids at the interface between the nematic LC 4'-*n*-pentyl-4-cyanobiphenyl (5CB) and an aqueous phase alters the nematic alignment from the planar to homeotropic (i.e., vertical) configuration, causing the optical texture of 5CB to change from dark to bright when observed under a polarized optical microscope (POM) with crossed polarizers [26]. With similar principles, LCs have been applied in the recognition of the orientation of immobilized proteins [27,28], the signal amplification of binding between proteins and immobilized peptides [29] and real-time monitoring of enzymatic reactions [30,31]. Thermotropic LCs of low cytotoxicity are used to support the growth of human embryonic stem cells, which induce the reorganization of extracellular matrix and alter the orientational order of LCs during growth and differentiation [32]. Moreover, the ordering of LCs may serve as a signature to distinguish between lipid bilayer-enveloped and nonenveloped viruses [33], and may be used to identify endotoxins released from Gram-negative bacteria for the detection and diagnosis of sepsis [34]. These findings demonstrate the potential of clinical applications with LC biosensing, which is advantageously rapid, label-free, low-cost, and may be developed as point-of-care (POC) diagnostics [20].

Among the various biomedical applications of LCs, studies of the immunodetection of specific binding between antigens and antibodies by LCs are relatively scarce. It is known that the uniform orientation of 5CB by rubbed films of covalently immobilized bovine serum albumin (BSA) is disturbed after interaction with anti-BSA IgGs [35]. Lyotropic LCs are also used to detect the immunocomplex formed between antibodies and immobilized antigens [36]. A quantitative LC-based microfluidic immunoassay has been developed to correlate the antibody concentration with the length of bright region in the LC texture resulting from the interaction of antibodies with immobilized antigens [37]. It has been also proposed that the optical texture of LCs is related to the concentration of proteins or antibodies, and there exists a critical concentration to induce the dark-to-bright response for each individual protein or antibody [38]. In a study on the LC-based immunoassay of hepatitis B, it is reported that the immunocomplex formed between hepatitis B surface antigen (HBsAg) and hepatitis B antibody (anti-HBsAg) disrupts the homeotropic alignment of 5CB, rendering the planar texture observed under crossed polarizing filters. Moreover, the detection limit of anti-HBsAg decreases from 150 nM to 15 nM when a secondary antibody specific for anti-HBsAg is added to increase the size of the immunocomplex and, in turn, creates greater disturbance in LC orientation [39]. Nevertheless, a large discrepancy in sensitivity exists between LC-based immunodetection and conventional label-based methods used clinically, which demands a detection limit of 10 ng/ml (or lower), corresponding to an antibody concentration of 0.067 nM. Therefore, improving detection sensitivity is urgently needed in the development of LC-based immunoassays.

In an attempt to enhance the sensitivity of LC-based immunodetection without the use of secondary antibodies for simplicity, we exploited a eutectic mesogenic mixture exhibiting large anisotropy in refractive index ($\Delta n = 0.333$ at 20 °C) in the detection of the cancer biomarker CA125. Presumably, a LC of higher birefringence responds more sensitively to the binding events of antigens and antibodies, thus pushing the LC-based immunoassay to a lower detection limit. Unlike the single-compound LC 5CB with a very narrow nematic range of merely ~11 °C and thus strongly susceptible to the ambient temperature, the intrinsically wider nematic range of a eutectic mixture also suggests the optical texture produced to be more stable and reproducible, making the LC-based immunodetection more clinically feasible. Our previous studies have shown that by using LCs with larger birefringence, the sensitivity of immunodetection was drastically enhanced compared to 5CB, and the detection limit was 0.01–0.1 $\mu\text{g/ml}$ for CA125, which was significantly lower than that of label-based fluorescence immunoassay [40]. It was proposed that by mixing the antigen and antibody without eliminating unbound or unreacted biomolecules through washing, signal loss can be avoided, and a simplified procedure for faster LC-based immunoassay can be established,

Table 1. Materials Properties of HTW and 5CB

Liquid crystal	Nematic range (°C)	Birefringence (at 589 nm)
HTW	< -30.0–95.0	0.333 (20 °C)
5CB	24.0–35.1	0.179 (25 °C)

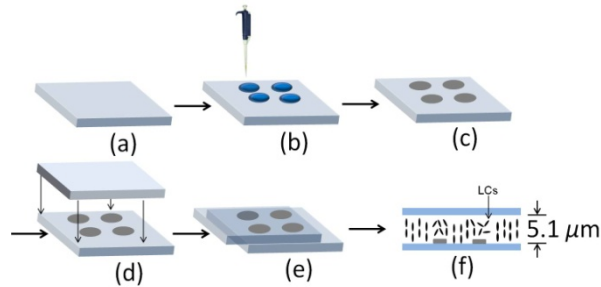


Fig. 1. Schematic illustration of sample preparation: (a) preparation of a DMOAP-coated slide, (b) dispensing the protein solution, (c) drying in shade to immobilize the protein, (d) dispensing 5.1- μm spacers on four corners then covering the slide with another DMOAP-coated slide, (e) sealing four corners with adhesive, and (e) introducing LC into the cell.

giving rise to a higher optical response using a high- Δn LC mixture compared to 5CB [41]. This study attempts to further demonstrate the detection sensitivity of the no-wash procedure in relation to reaction time and in the presence nonspecific antibodies. As the change in optical textures of LCs can only provide qualitative description of the immunoreaction, this study is also the first to propose a quantification method for the optical response of LCs.

2. Experimental

2.1 Materials

Display-grade glass slides (15 mm \times 20 mm) were received from Mesostate (Taiwan). Ethanol and the aligning agent *N,N*-dimethyl-*n*-octadecyl-3-aminopropyltrimethoxysilyl chloride (DMOAP) dissolved in methanol were both purchased from Acros Organics. Antibodies (150 kDa) against CA125 and spermidine/spermine N^1 -acetyltransferase (SSAT) were provided by Santa Cruz Biotechnology. Recombinant human CA125 (~110 kDa) was manufactured by R&D Systems. BSA (66 kDa) was obtained from Sigma–Aldrich. The high- Δn nematic LC designated HTW is a multicomponent LC produced by HCCH (China). The typical nematic LC 5CB purchased from Daily Polymer (Taiwan) was also employed as a reference. Table 1 comparatively displays some physical properties of both HTW and 5CB. Water was purified and deionized with an RDI reverse osmosis/deionizer system.

2.2 Surface modification of glass slides with DMOAP

Glass slides were cleaned successively in soap water, DI water and ethyl alcohol by ultrasonication, with each step lasting 15 min. The slides were then dried under a stream of nitrogen and baked at 100 °C for 10 min. After the cleaning process, the slides were immersed in a 1% (v/v) DMOAP solution for 15 min, followed by washing with DI water under ultrasonication for 10 min, drying again with nitrogen, and baking at 100 °C for 15 min, subsequently. Afterwards, the slides were left in the oven for 6 h to cool down to room temperature. The DMOAP coating thus formed a network that induced the homeotropic alignment (i.e., aligning perpendicularly to the substrates) of the LC molecules.

2.3 Sample preparation

Anti-CA125 antibody was directly mixed with CA125 antigen and the mixture was shaken on a vortex mixer for 6 h except for the time-evolved experiment. The mixture was then dropped on the substrate. After dried in shade to form a thin film of protein, spacers of 5.1 μm in size

were dispensed on the four corners of the glass slide. Then another substrate was covered to form an empty cell with a uniform cell gap as determined by the spacers. HTW or 5CB was infiltrated into the cell by capillary action at room temperature (Fig. 1). In conventional immunoassays, an antibody is first immobilized on a substrate and an antigen is then layered on the antibody [40]. In this study, the antigen and antibody were mixed prior to immobilization to simplify the procedure as well as to explore other possible experimental design for LC-based immunoassay.

2.4 Optical observation and quantitative analysis

Optical textures of HTW and 5CB were examined under a POM (OLYMPUS BX51) in the transmission mode. All of the images were captured with an exposure time of 16 ms. In control experiments, CA125 antigen, anti-CA125 antibody, BSA, anti-SSAT antibody, mixtures of CA125 antigen and anti-SSAT antibody were separately immobilized on treated glass slides for LC detection. To obtain qualitative results, QT, a freeware based on C++, is exploited. We first quantize each observed image by summing up its total RGB value within a circular region of 700 pixels in diameter, which is slightly larger than the size of the sample droplet, then divide the sum by its area. The obtained value is referred to in this study as the "relative intensity (RI)." At each concentration of antigen, we calculate the averaged RI of at least 16 samples as well as the corresponding standard deviation σ , where σ is considered as the statistical (and also the major) error in this study. In the first part of our study, we calculate the p -value of RI to compare the 5CB and the HTW results. Then, to determine the detection range of immunoreaction, we calculate the p -value of immunocomplex with respect to the case when only antigen is present at the same concentration. The range of concentration with p -value smaller than 0.001 is regarded as the detection range.

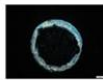
3. Results and discussion

3.1 Detection of protein or antibody with HTW or 5CB

LC molecules were aligned perpendicularly to the glass surface with the help of DMOAP. In the absence of proteins, the image under the microscope with crossed polarizers appeared completely dark. When protein samples were present, bright spots were observed. This phenomenon can be understood as the result of uniaxiality of the LCs used. When the optical axis is parallel to the light path, the plane of the polarized light is not rotated, and thus light is not transmitted by the second polarizer. In the presence of immobilized proteins, the alignment of LCs is disturbed, making the local optical axis no longer parallel to the light path. In this case, the plane of the polarized light is rotated, and thus can be transmitted by the second polarizer; therefore, bright spots (i.e., optical textures) can be seen [42]. This rotating effect can be enhanced when a mesogen with larger optical birefringence is exploited.

Figure 2 shows the optical textures of either 5CB or HTW with 0.01, 0.1 and 1 $\mu\text{g}/\text{ml}$ (1 μl per droplet) of CA125 antibody and antigen alone. For 5CB, the optical texture was undetectable (or remained dark) when the concentration of CA125 antigen or antibody was below 0.1 $\mu\text{g}/\text{ml}$, while in the case of HTW, the optical texture was still discernible at an antigen or antibody concentration of 0.01 $\mu\text{g}/\text{ml}$. The t -tests all yield p -value below 0.001, indicating the difference are well discernable. Similar findings were observed in the presence of BSA or anti-SSAT antibody, implying that the optical signal produced by the immobilized protein or antibody was better amplified with HTW than 5CB. These results support our hypothesis that mesogens exhibiting higher optical birefringence enhance the sensitivity of protein or antibody detection.

(a) CA125 Ag ($\mu\text{g/ml}$)	HTW	Intensity (arb. units)	5CB	Intensity (arb. units)	<i>p</i> -value
1		132.0 ± 22		28.4 ± 6	1.1 × 10 ⁻¹¹
0.1		22.0 ± 2		15.8 ± 1	1.3 × 10 ⁻¹¹
0.01		20.8 ± 2		15.1 ± 1	2.0 × 10 ⁻¹¹

(b) CA125 Ab ($\mu\text{g/ml}$)	HTW	Intensity (arb. units)	5CB	Intensity (arb. units)	<i>p</i> -value
1		101.9 ± 33		21.5 ± 11	3.4 × 10 ⁻⁷
0.1		44.1 ± 11		17.1 ± 1	5.1 × 10 ⁻¹⁰
0.01		30.2 ± 10		21.2 ± 2	1.0 × 10 ⁻³

(c) SSAT ($\mu\text{g/ml}$)	HTW	Intensity (arb. units)	5CB	Intensity (arb. units)	<i>p</i> -value
1		212.8 ± 67		119.2 ± 23	3.5 × 10 ⁻⁶
0.1		22.5 ± 6		6.3 ± 1	6.5 × 10 ⁻⁷
0.01		16.1 ± 2		5.7 ± 2	7.5 × 10 ⁻¹²

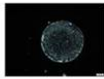
(d) BSA ($\mu\text{g/ml}$)	HTW	Intensity (arb. units)	5CB	Intensity (arb. units)	<i>p</i> -value
1		270.1 ± 26		146.8 ± 33	2.5 × 10 ⁻¹⁷
0.1		73.7 ± 17		12.1 ± 4	1.4 × 10 ⁻⁸
0.01		22.3 ± 6		4.8 ± 1	3.8 × 10 ⁻⁷

Fig. 2. Comparison of optical textures of HTW and 5CB in the presence of (a) CA125 antigen, (b) anti-CA125 antibody, (c) BSA, and (d) anti-SSAT antibody.

3.2 Temperature range of HTW and 5CB

The phase transition temperature is different for every mesogen. For 5CB, the LC phase exists in the range of 24–35 °C, while for eutectic mesogen HTW, the LC phase exists from below –30 to 95 °C as presented in Table 1. In this experiment, a Linkam T95-PE temperature control system was used to control the temperature between –40 °C and 120 °C. We dropped 2 μ l of 1- μ g/ml anti-CA125 antibody on substrates to compare the result of 5CB and HTW. For 5CB we measured the optical textures from –10 to 35 °C as shown in Fig. 3(a). Below 23 °C, 5CB is in the crystalline phase, rendering the optical texture (with extremely high noise) from the protein undetectable. Above 35 °C, 5CB is in the isotropic phase with no birefringence to transduce the signal; no signal was observed. The functioning temperature spans only 12 °C. For HTW (Fig. 3(b)), clear signal can be seen from –30 to 108 °C. The temperature range is as large as 138 °C, confirming the merit of wide temperature detection by using HTW.

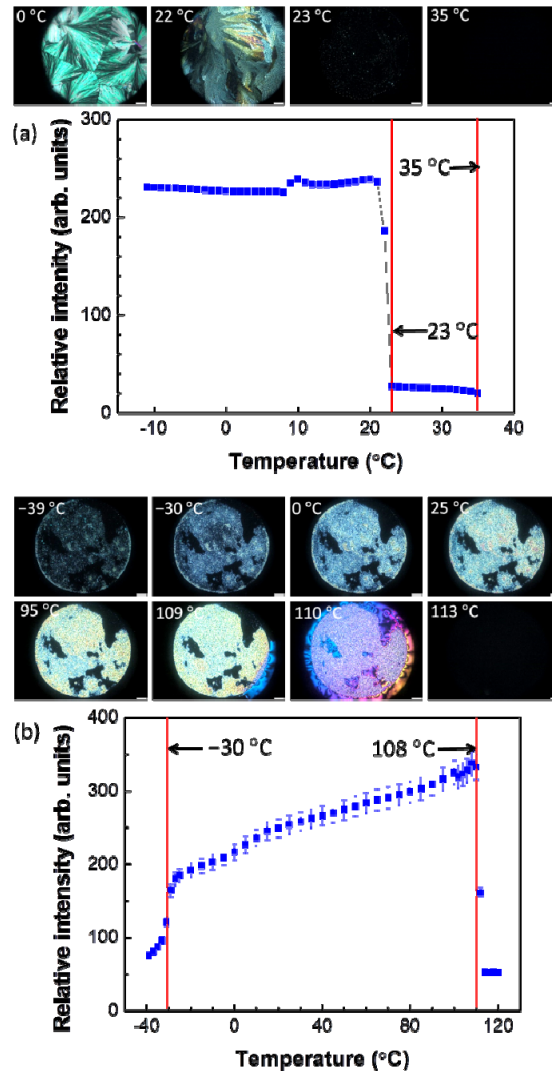


Fig. 3. Optical textures and their relative intensities of (a) 5CB and (b) HTW in the presence of 1- μ g/ml anti-CA125 antibody at different temperatures.

	0.0001 ($\mu\text{g/ml}$)	0.001 ($\mu\text{g/ml}$)	0.01 ($\mu\text{g/ml}$)	0.1 ($\mu\text{g/ml}$)	0.5 ($\mu\text{g/ml}$)	1 ($\mu\text{g/ml}$)
CA125 antibody						
CA125 antigen						
CA125 immuno-complex						

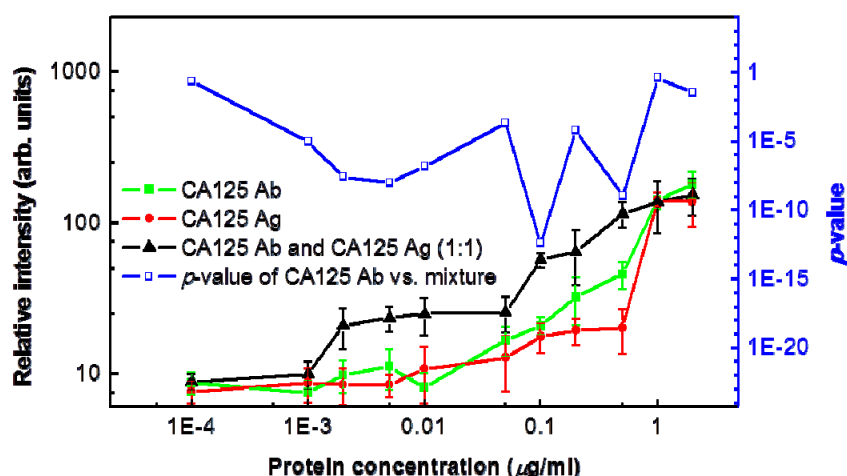


Fig. 4. Optical textures and their relative intensities of mixed CA125 antibody and antigen (1:1 in volume) at various concentrations and the corresponding p -value.

3.3 Immunodetection of specific binding between CA125 antibody and antigen with HTW or 5CB

We then mixed 0.1–2000-ng/ml anti-CA125 antibody with identically concentrated CA125 antigen of the same volume to allow the formation of immunocomplex between the specific antigen/antibody pairs. The mixture was dispensed at $2 \mu\text{l}$ per droplet on DMOAP-coated glass substrate and air-dried at room temperature. Proteins and antibodies are usually immobilized and dried on glass or plastic substrates in label-based immunoassays, and can be stored for several months without losing binding activity. As antigens and antibodies are complexed through multiple noncovalent interactions such as hydrogen bonds, electrostatic interactions, hydrophobic interactions and van der Waals forces, several hours (at most 6 h in this study) of drying should have minimal effect on the stability of the CA125 immunocomplex.

When detected with HTW, the CA125 antigen/antibody mixture resulted in a brighter spot under a POM, compared with that of same-concentrated CA125 antigen or antibody alone (Fig. 4). These results suggest that the larger size of the CA125 immunocomplex, in comparison with CA125 antigen or antibody alone, induced more significant disruption of LC alignment (Fig. 5). This method of immunodetection can thus discern between immunocomplexes and unbound antigens or antibodies, and a detection region with the p -value smaller than 0.001 was determined to be 1–500 ng/ml without the use of secondary antibodies. At higher concentrations, the signal was saturated and resulted in a plateau-like

behavior. In a parallel study conducted with 5CB, the CA125 immunocomplex was barely detectable (Fig. 6), which provides further evidence for enhanced immunodetection sensitivity by HTW.

When the optical texture of anti-CA125 antibody or CA125 antigen was compared in Figs. 2 and 4, it was found that the distribution of these biomolecules varied in individual experiments. Uneven distribution of the sample usually occurs when low concentrations of the anti-CA125 antibody and/or CA125 antigen were present, resulting in LC signals with areas smaller than the original drop size. Because the protein samples were air dried under room temperature, and the time required for drying may be affected by both temperature and humidity, the uncontrolled drying rate may thus contribute to the uneven distribution of proteins on the DMOAP-coated slides. Nevertheless, the relative intensities of 0.01-, 0.1- and 1- $\mu\text{g}/\text{ml}$ CA125 antigen or anti-CA125 antibody were of the same order of magnitudes in both figures, indicating that although the CA125 antigen or antibody molecules in each sample were distributed in different patterns in Figs. 2 and 4, the relative intensities of the resulting LC signal were quite consistent.

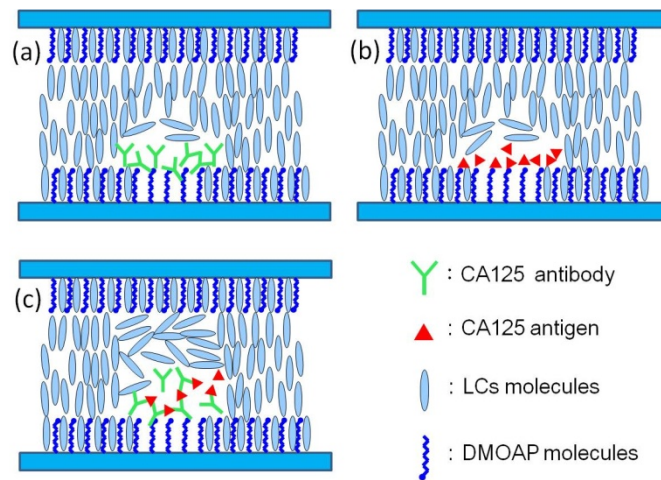


Fig. 5. Schematic of mesogenic orientation in cells with (a) anti-CA125 antibody immobilized and DMOAP coated on the substrates, (b) CA125 antigen immobilized and DMOAP coated, and (c) CA125 immunocomplex immobilized on the DMOAP coating.

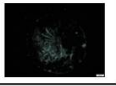
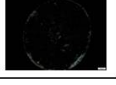
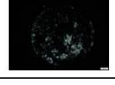
	CA125 antibody	CA125 antigen	CA125 immuno-complex	<i>p</i> -value
HTW				1.12×10^{-9}
5CB				4.15×10^{-3}

Fig. 6. 0.5- $\mu\text{g}/\text{ml}$ mixture of CA125 antibody and antigen comparing with only antigen/antibody alone using 5CB and HTW.

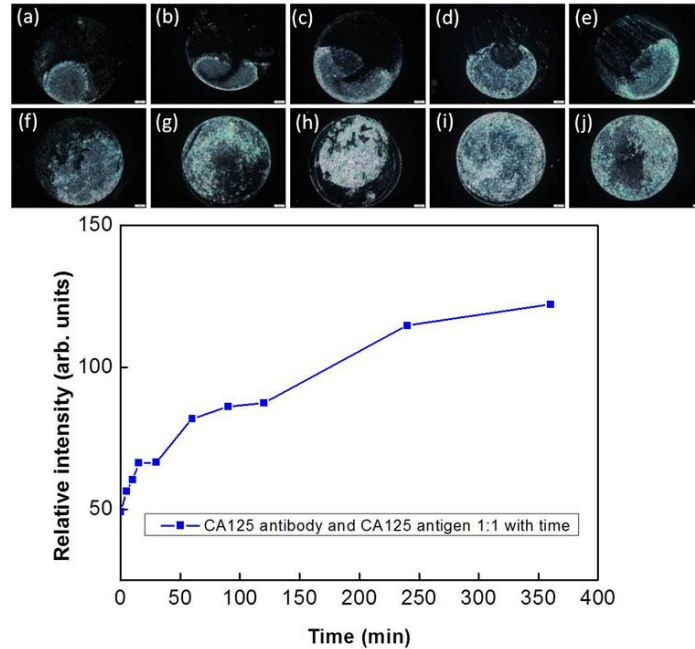


Fig. 7. Change in optical texture of HTW with reaction time in the presence of a mixture of 0.5- $\mu\text{g}/\text{ml}$ anti-CA125 antibody and 0.5- $\mu\text{g}/\text{ml}$ CA125 antigen. The mixture was allowed to react in a test tube for (a) 0 min, (b) 5 min, (c) 10 min, (d) 15 min, (e) 30 min, (f) 60 min, (g) 90 min, (h) 120 min, (i) 240 min and (j) 360 min before immobilization on DMOAP-coated glass substrates and LC cell assembly. The result indicated that the system reaches stability in 240–360 min.

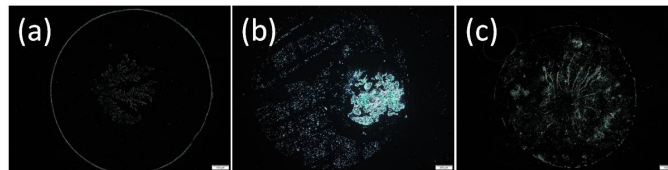


Fig. 8. Optical textures of HTW in the presence of (a) 0.1- $\mu\text{g}/\text{ml}$ CA125 antigen mixed with 0.1- $\mu\text{g}/\text{ml}$ anti-SSAT antibody, (b) 0.1- $\mu\text{g}/\text{ml}$ CA125 antigen mixed with 0.1- $\mu\text{g}/\text{ml}$ anti-CA125 antibody, and (c) 0.1- $\mu\text{g}/\text{ml}$ anti-SSAT antibody.

We further investigated time dependency of the change in optical texture of HTW over time. Only in this experiment, instead of dried in shade, droplets on substrate were dried at 30 °C on a hot plate to achieve better control of reaction time. As revealed in Fig. 7, the brightness of the optical texture increased with increasing reaction time and reached a plateau within 60–90 min and leveled off after 240–360 min. The time-course data therefore indicates that a prolonged reaction time of CA125 antigen with anti-CA125 antibody may increase the amount of antigen–antibody immunocomplex, thereby creating greater disturbance in the alignment of LCs as well as higher intensity in optical texture.

3.4 Discrimination between specific and nonspecific antibodies

To test the specificity of immunodetection with HTW, 0.1- $\mu\text{g}/\text{ml}$ CA125 antigen was reacted with anti-CA125 antibody or anti-SSAT antibody of the same concentration for 6 h. As shown in Fig. 8, the optical texture is of relative intensity 7.7 ± 1.1 for mixture of anti-SSAT antibody and CA125 antigen (Fig. 8(a)). This is significantly weaker than 55.0 ± 8.4 as obtained for the mixture of CA125 antigen and antibody (Fig. 8(b)). When only anti-SSAT antibody is present, the relative intensity is 28 ± 7 (Fig. 8(c)), close to the results with only

CA125 antigen/antibody. Disruption of LC alignment was significant only in the presence of both CA125 antigen and CA125 antibody, suggesting that the CA125 immunocomplex was formed. The nearly dark texture of HTW in the presence of both anti-SSAT antibody and CA125 antigen indicates that no immunocomplex was formed between nonspecific antigens and antibodies. It is therefore evident from these results that LC immunodetection is capable of discriminating between the presence of specific and nonspecific antibodies.

4. Conclusions

We have demonstrated that the sensitivity of LC-based immunoassays can be promoted by applying a eutectic nematic mixture with larger birefringence ($\Delta n = 0.333$ for HTW in this study). The inherently wide nematic range (> 125 °C for HTW) and very high nematic phase stability (95.0 °C for HTW) in contrast with a single-compound nematic, *e.g.*, 5CB, are advantageous for reliable label-free immunodetection. The detection region of the cancer biomarker CA125 is determined to be 1–500 ng/ml without ambiguity, which is sufficient for clinical diagnosis. The presence of specific antibodies and formation of immunocomplex can be clearly distinguished from nonspecific antibodies by inspecting the optical textures of LCs. With elevated sensitivity and reliability, immunodetection using high-birefringence LC mixtures is therefore considered truly a label-free, sensitive and specific technique that may serve as an alternative to conventional immunoassays.

Acknowledgments

The authors would like to thank Professor Jhi-Joung Wang, Drs. Sheng-Hsien Chen and Chien-Feng Li as well as Ms. Li-Ching Wu of Chi Mei Medical Center for providing technical advices. This work was supported by the Ministry of Science and Technology, Taiwan, under grant Nos. 101-2112-M-009-018-MY3 and 101-2314-B-309-001-MY3.